Does the pyloric neuron exhibit resonance?

Karina Aliaga

UBMTP

December 10, 2008

I. Abstract

Many experiments have been performed on the crab *Cancer Borealis* with regards to determining the existence of resonance in neurons found in the STG. Membrane resonance is a property that many neurons exhibit where there is high impedance at a preferred frequency. If membrane resonance exists, then the neuron is capable of differentiating between its inputs thereby been able to recognize an oscillatory input at a preferred frequency where the largest response will be produced. This paper describes the different methods applied to a pyloric neuron in order to determine the existence of resonance in the cell.

II. Introduction

Numerous studies have been made on the crab *Cancer borealis*, which is a large red deep-water crab of the eastern coast of North America. For purposes of the experiment, the crab *Cancer borealis* goes through a two step dissection process which will be discussed later on. At the completion of the dissection process, the crustacean stomagastric nervous system (STNS) is extracted. The STNS is composed of four ganglia including the commissural ganglia (CoGs), the esophageal ganglion (OG) and the stomatogastric ganglion (STG) as shown in Figure 1. For purposes of the experiment, we are going to focus on the STG. The STG is composed of thirty neurons from which eleven to fourteen neurons belong to the pyloric network. The pyloric network is composed of motor neurons with the exception of the AB neuron. These neurons send signals that are transmitted to the digestive muscles of the crab through the corresponding neuronal axons (Warrick 1992). In our experiment, we primarily focus on understanding signals involved in the pyloric neuron (PY).

Many studies show that some neurons are capable of exhibiting resonance. Resonance is a property that characterizes the frequency at which neurons respond best to inputs of injected current (Hutcheon 2000). In a rhythmic system, a post-synaptic neuron receives repetitive synaptic current at a given frequency. Consequently, the post-synaptic neuron will respond best when the synaptic current is at its resonant frequency. Since at the resonant frequency the voltage response is the greatest, an action potential has the best chance of being produced.

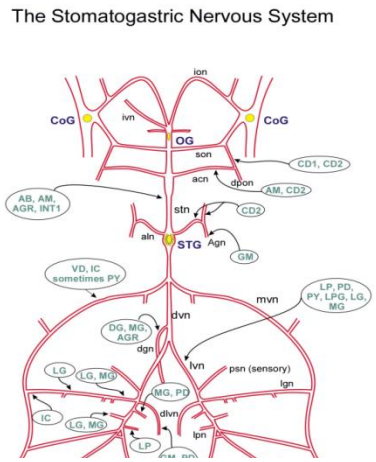

Figure 1: STNS as it should appear after the fine dissection.

In addition to understanding the concept behind resonance, it is important to know how does resonance arises from a biological perspective. Membrane resonance arises from the interplay between the cell's active and passive property. There are two mechanisms involved in these properties; one of these mechanism blocks the voltage responses at low frequencies meanwhile the other mechanism blocks the voltage responses at high frequencies. In every cell, the semi-permeable cell membrane separates the interior of the cell from the extracellular liquid therefore acting as a capacitor with its corresponding resistance. Consequently, the outer membrane serves as a filter that allows the voltage responses at low frequencies to go through and blocking those at high frequencies. This demonstrates the characteristic of a low pass filter which is found in every cell including the pyloric neuron (Hutcheon 2000).

By a cell portraying the passive property, it does not guarantee that it will produce resonance since the cell must also exhibit an active property as well. The active property is characterized by the cell's block of voltage responses at low frequencies therefore it is referred as a high pass filter. In addition, there must be a significant voltage change in response to the input current. Also, it must activate slowly relative to the membrane time constant. In other words, the activation time constant for the voltage gated current should be slower than the membrane time constant in order for resonance to be produced. The characteristics of an active property are found in a hyperpolarized current (I_h) which will be referred later on. If all of these conditions are met, then resonance should be created at the intermediate frequencies where inputs of current will produce voltage changes at frequencies too high to be opposed by the I_h current and too low to be counteracted by the passive properties of the membrane. If there is a lack of a gap between both frequencies then this will result in the absence of resonance (Hutcheon 2000).

Mathematically, resonance is defined as a property of impedance. Impedance is the frequency dependent relationship between the amplitudes of oscillatory signals (Hutcheon 2000). Recalling Ohm's law, resistance is defined as voltage divided by current however; these factors are dependent on time and not by frequency such as impedance. Consequently, we use a method called fast Fourier transforms (FFT) to fix this problem. The fast Fourier transform is a mapping of a function as a signal that is defined in one domain as time into another domain as frequency where the function is represented in terms of sines and cosines. As a result, impedance is calculated by taking the fast Fourier transform of the voltage response over the fast Fourier transform of the input current. The current used for purposes of the experiment is a zap current which is just a signal that goes through many frequencies over time. Each frequency in the input is isolated briefly in time so that the frequency response can be analyzed.

Many neurons in the STG have been studied in order to determine if resonance exits. If resonance is found, than this means the neuron is able to differentiate between its inputs so that it can recognize an oscillatory input at a preferred frequency where the largest response will be produced. Consequently, many experiments were performed on the pyloric neuron in order to determine if there exists a preferred frequency by this cell.

III. Methods

A. Dissection Process

All of the experiments were performed on the crab *Cancer borealis,* a large red deep-water crab of the eastern coast of North America. Before it goes through the dissection process, the crab is stored in a tank that resembles an artificial seawater environment. Once prepared for the dissection, the crab is placed in ice for approximately half an hour in order to anesthetize it and make the dissection process, an easier one. During the crude dissection, the stomach of the crab is extracted in a process that takes approximately fifteen minutes. Following that procedure, the stomatogastric nervous system is extracted in a process called fine dissection. The purpose of this dissection is to take the STNS and place it in a Petri dish which should resemble Figure 1. In addition, the STG is identified and desheathed in order to expose the cells around the ganglion where the pyloric neuron will be encountered. There are approximately twenty four to thirty neurons found surrounding the ganglion, but only five of them are the pyloric neurons, therefore a final procedure is required in order to properly identify the PY neuron.

In order to identify the PY neuron, vaseline wells in the Petri dish are built around the lateral ventricular nerve (*lvn*) and the medial ventricular nerve (*mvn*). In addition, the stomatogastric nervous system is submerged in a saline solution composed of 11 mM KCl, 13 mM $CaCl_2 \cdot 2H_2O$, 26 mM $MgCl_2 \cdot 6H_2O$, 440 mM NaCl, 11.2 mM Trizma base, and 5.1 mM Maleic acid. The saline solution has to be within a temperature that lies between 10 and 13 º C as well as having a pH of 7.4-7.5 which will permit the survival of the STNS (cancer.rutgers.edu). The vaseline wells built around the nerves will contain two electrodes around it. The first electrode is placed anywhere outside the vaseline well while the second

electrode is placed inside the vaseline well. Both of these electrodes are utilized in the calculation of the difference in voltage response once the zap current has been applied. After placing the electrodes in the Petri dish, microelectrodes must be used to identify the pyloric neuron. Before using the microelectrode to pierce the neuron, it must be filled with a 0.6 M K_2SO_4 and 0.02 M KCl solution (cancer.rutgers.edu). The microelectrodes are then attached to the manipulators in order to accurately pierce the specified neuron.

By performing an intracellular recording and an extracellular recording, the pyloric neuron can be correctly identified. First, an extracellular recording of the *lvn* and *mvn* is performed using a differential AC amplifier. Secondly, by using an axoclamp amplifier the intracellular recording of the pyloric neuron is accomplished. As observed in the figure below, the intracellular recording will show repetitive burst of the pyloric neuron which should be in phase with the PY bursts observed in the extracellular recording of the *lvn*. Since there is another neuron called VD that portrays these same characteristics, the extracellular recording of these PY bursts should be out of phase with the extracellular recordings of the *mvn*.

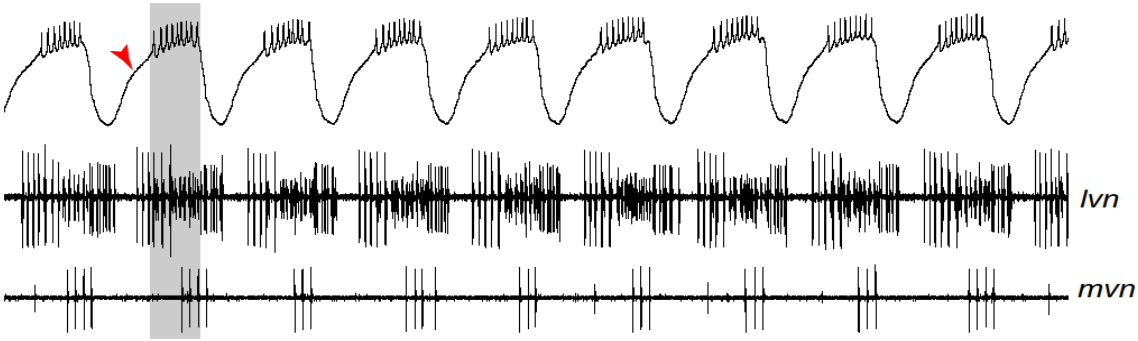

Figure 2: The first bursts shown are from the intracellular recording of the pyloric neuron. It is followed by the extracellular recordings of lvn and mvn.

B. Current Clamp Procedure

The experiment is performed by a process called current clamping. This process involves obtaining two microelectrodes and inserting them in to the pyloric neuron. To ensure the presence of these microelectrodes in the preferred neuron, the cell is depolarized through one electrode and the response is recorded through the second electrode. By analyzing the response, the presence of the microelectrodes in the pyloric neuron can be verified. Consequently, a current is injected through an electrode with a low resistance and the voltage is measured through the second electrode with a high resistance.

Once the current clamp procedure is set up correctly, the next step is to stop the neuromodulators from entering the stomagastric ganglion (STG). By adding 10^{-7} mM tetrodotix to the Petri dish, the neuromodulators will be attenuated since TTX blocks action potentials in nerves by binding to the pores of the voltage-gated, sodium channels in the nerve cell membrane. As a result, the pyloric neuron shows no rhythm due to the addition of this chemical.

C. Existence of hyperpolarized current (I_h)

In the pyloric neuron we can find different kinds of ionic currents, however we focus on the hyperpolarized current (I_h) since it possesses an active property required for resonance to exist. If an active property exists in the neuron then it must serve as a high pass filter. To prove the existence of the hyperpolarized current, a step current is injected into the cell which ranges from 1nA to 7nA with increments of 1nA. This procedure is performed using the software called Scope (Nadim 2006). By recording the voltage response due to the inserted current, the sag as observed in Figure 3 should be produced.

After the presence of the I_h current has been verified, a zap current is injected using a microelectrode. Since different step currents were injected in the previous step, it can be observed which step current produced the most visible sag confirming the presence of I_h. Consequently, this value in nanoamperes is used when injecting the zap current so that the voltages response obtained will be the one at which I_h activates.

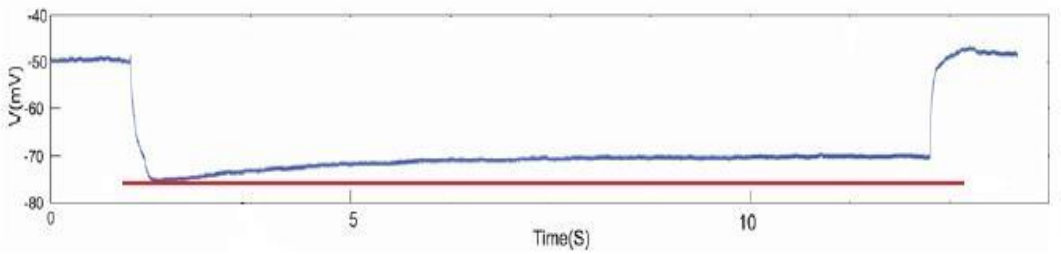

Figure 3: Figure 3: It demonstrates the voltage response due to an injected step current, but most importantly it shows the sag (the upward deviation of the step current from the red line) thereby proving the existence of Ih.

In addition to using the step functions as a procedure to proving the existence of I_h, Cesium Chloride was used as well. Approximately, 10 mM CsCl was added to the Petri dish with the purpose of blocking this hyperpolarizing current. Theoretically, if resonance does exist, the appropriate voltage response should be reached before the addition of Cesium Chloride, however; this respond should disappear after adding this I_h blocker and similarly come back as the Cesium Chloride is washed out. This procedure was confirmed experimentally and will be discussed later on.

D. Dynamic Clamp Technique

The Dynamic Clamp technique allows for the injection of an artificial current that resembles a current that would flow through a real membrane. Consequently, an artificial I_h current can be injected into the pyloric neuron by using equation (1). In this artificial I_h, the conductance applied can be changed.

$$I(V,t) = \bar{g}m(V - E_{rev}) \quad (1)$$

In this equation, $\bar{g}$ represents the maximum conductance, m is the activation gate and E_{rev} is the reversal potential.

Experimentally, the following parameters are used:

Dynamic Clamp Protocol	
V (voltage)	-50mV
K (slope)	4.0
T_{low} (Time constant)	270mS
T_{high} (Time constant)	1800mS

IV. Experimental Results

In order to determine the presence of I_h in the pyloric neuron, as mentioned before, a step current was injected and we looked for a resulting sag current. However, at specific step currents, the sag becomes more visible than others. Experimentally, step currents that ranged from -1nA to -7nA were injected and consequently, different I_h sag responses were observed. The figure below shows the different I_h sag responses due to the different input of currents, thereby demonstrating that when a step current of -7nA is used, the pyloric neuron depolarizes thus it producing the greatest sag response. However, when the injected current ranges -3nA to -5nA, there is no visible sag due to the fact that I_h only activates sufficiently to inhibit the neuron from further hyper polarization.

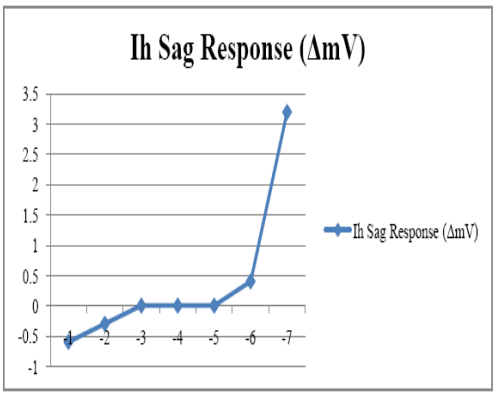

Figure 4: Ih sag response due to changes in injected current ranging from -1nA to -7nA.

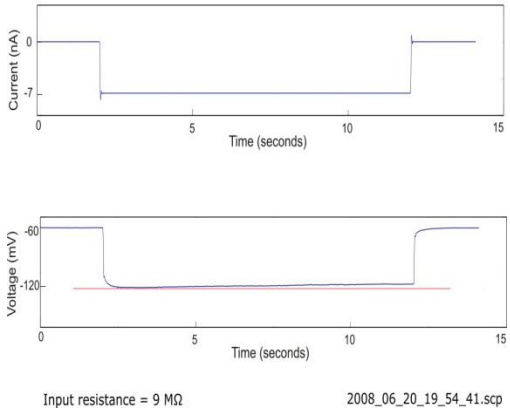

Figure 5: The first graph shows the 7nA of injected current follow by its voltage response.

Consequently, we want to use a step current that clearly shows the I_h sag response since it means that I_h gets activated. In the experiment, -7nA of injected current showed a visible sag response as observed in Figure 5. In addition, this current injection drops the voltage to -120mV which is lower than when I_h usually activates.

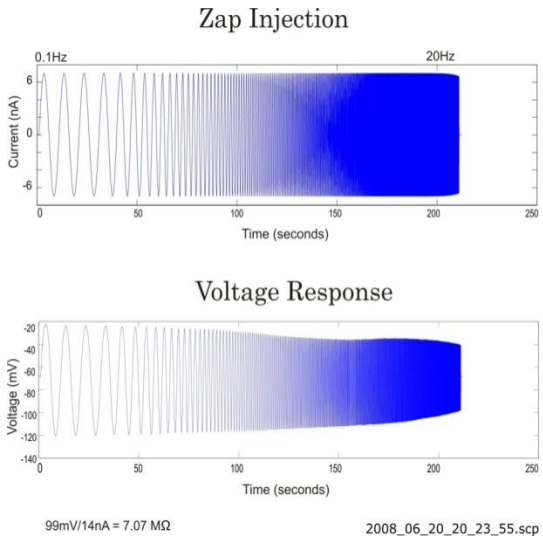

Figure 6: The graph on the top shows the injected zap current, followed by its corresponding voltage response when using the current clamping technique.

For every experiment performed, a zap current was injected at different amplitudes in order to find the best voltage response. In addition, the zap current ranged in frequency from 0.1Hz to 20Hz and it was run for 180 seconds with 3 pre-cycles. Since the presence of I_h is most visible at 7nA, we injected a zap current of -7nA and recorded its voltage response as seen in Figure 6.

In Figure 6. the voltage response due to the injected zap current is observed to range from -20mV to -120mV. As the time increases, the change in voltage decreases accordingly.

After performing many experiments, the data was analyzed using two different methods in order to compare the results. Both of these methods which for our purposes will be referred to as Method1 and Method2 are run in a program called Matlab. The idea behind Method1 is to use the data from the injected current and find a baseline that will serve a midpoint of these data. Since the injected current is a zap current then it is composed of sine curves, therefore this method takes one cycle at a time and collects the intersection point of the curve with the baseline. This process is repeated with the corresponding data for the voltage response. By having both measurements, resistance can be calculated for each cycle by simply following ohm's law. This procedure is repeated for the duration of the experiment and different resistance points are collected which are plotted for further analysis. Figure 7 shows the impedance graph using Method1 made out of different resistance points. In addition, Method2 is introduced in order to compare the data results and increase the accuracy of the conclusions. Method2 uses

fast Fourier transforms in order to calculate impedance. This method involves taking the injected current and applying FFT to convert its domain from time to frequency. This procedure is similarly done with the voltage response. As a result, impedance is calculated by taking the FFT of voltage and divided by the FFT of the injected current whose plot of impedance vs. frequency produces a smooth graph unlike Method1.

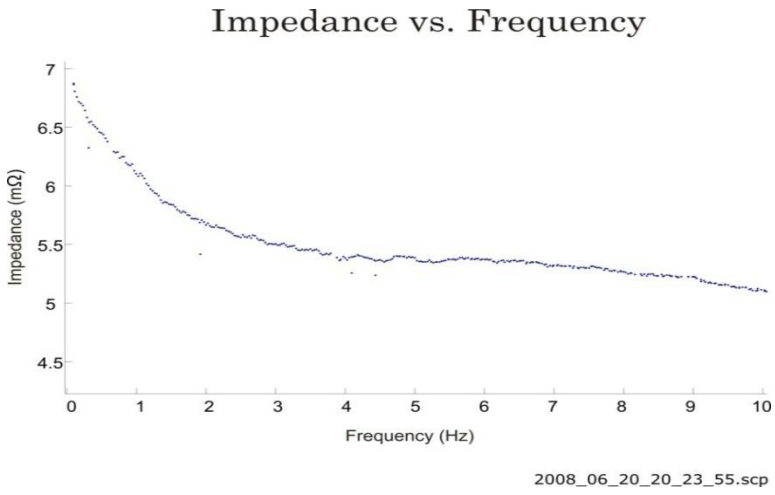

Figure 7: This shows the Impedance vs. Frequency graph using Method1.

Resonance as mentioned before is a property in which a neuron responds best to inputs of injected current. Consequently, if resonance were present it would appear as a bump in the graph reflecting a preferred frequency. However, Figure 7 shows no visible peak therefore resonance is not perceived in this experiment. Nonetheless, in order to assure this conclusion cesium chloride was used to block the I_h. If resonance in fact did not exist, upon the addition of CsCl, there would be no significant difference in the Impedance vs. Frequency graphs as observed in the experiment.

The procedure involving the addition of CsCl involved a two step process. First, a -6nA of injected current was required to active Ih. The voltage response recorded as observed in

Figure 8 shows the voltage ranging from -20mV to -140mV. In addition, the impedance vs. frequency graph using both Method1 and Method2 were performed as well as shown in Figure 9.

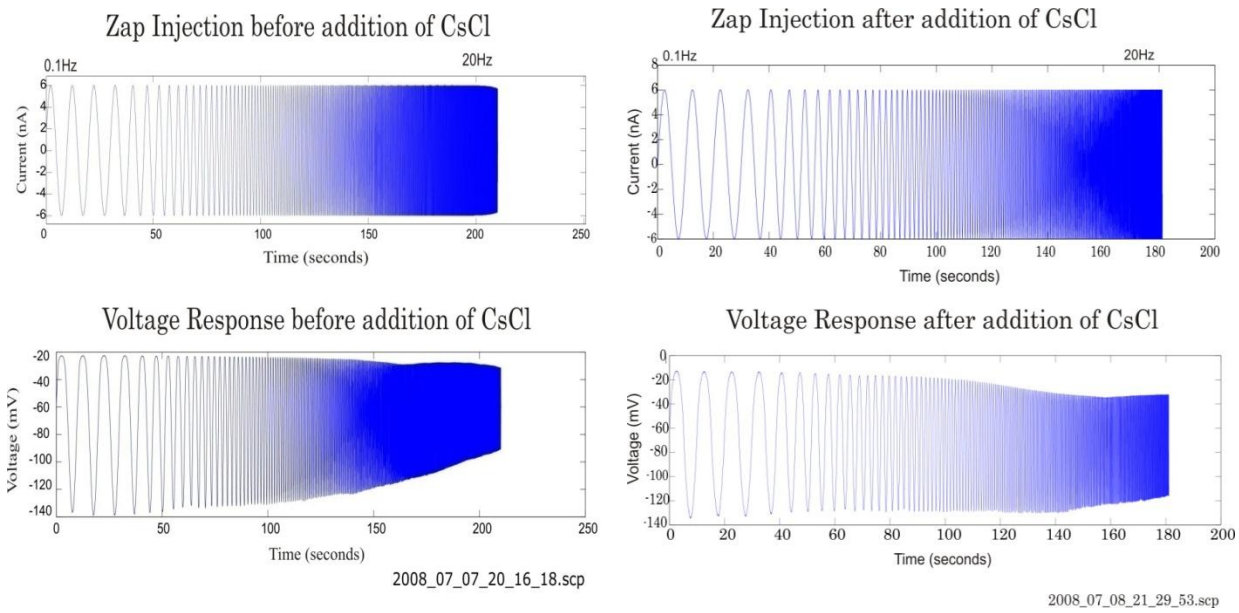

Figure 8: The graphs shown above display the voltage responses before and after the addition of CsCl.

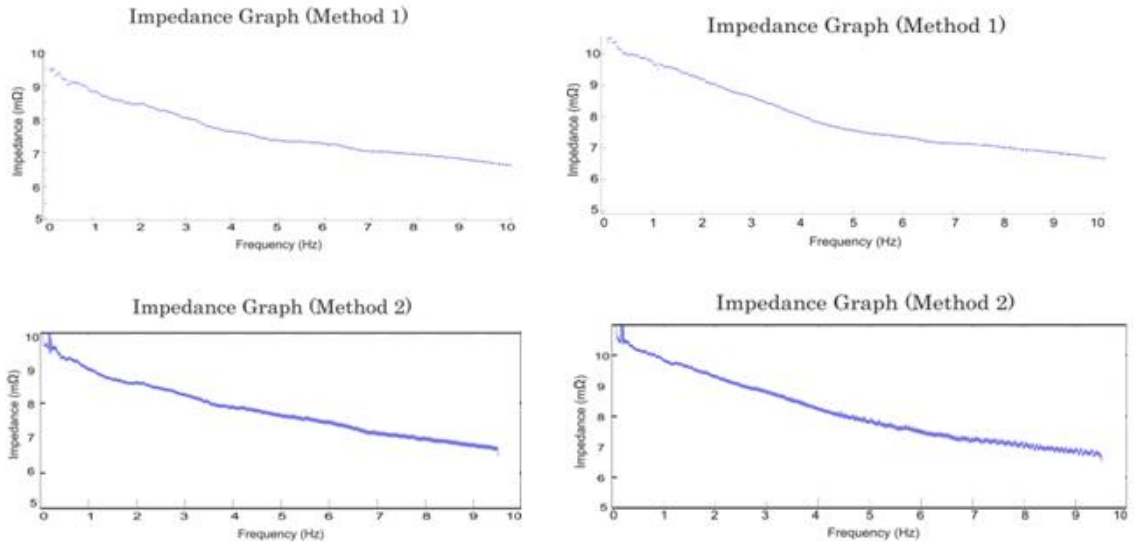

Figure 9: The graphs on the left show the Impedance vs. Frequency for before the addition of CsCl. The graphs on the right show the Impedance vs. Frequency for after the addition of CsCl

Secondly, 10mM of CsCl was added to the Petri dish and 6nA of injected current was applied thereby giving the voltage response observed in Figure 8. By comparing both voltage responses,

there is no significant change that could show a signature of resonance in the pyloric neuron. However, to clarify these results, the impedance vs. frequency graphs using both Method1 and Method2 were created for the data gathered before and after the addition of CsCl as shown in Figure 9. Even though, the I_h current was blocked by using CsCl, there was no significant difference in the impedance graph thereby confirming that resonance is not presence in the pyloric neuron. According to the above graphs, impedance decreases as frequency increases and there is no preferred frequency found in this neuron.

In order to explain the reasons for not finding resonance in the pyloric neuron, a new procedure was conducted called dynamic clamping. In order to be able to compare the effect of this procedure data was gathered for before and after the addition of this artificial current. For the control experiment, -1nA of injected current was required for the activation of Ih since it hyperpolarize the neuron to approximately -90mV as observed in figure 10. Similarly, an artificial Ih current with a conductance of 30µS was applied and it hyperpolarized the neuron to -70mV. In addition figure 10 the Ih sag can be clearly seen in the voltage response upon the addition of the artificial Ih current.

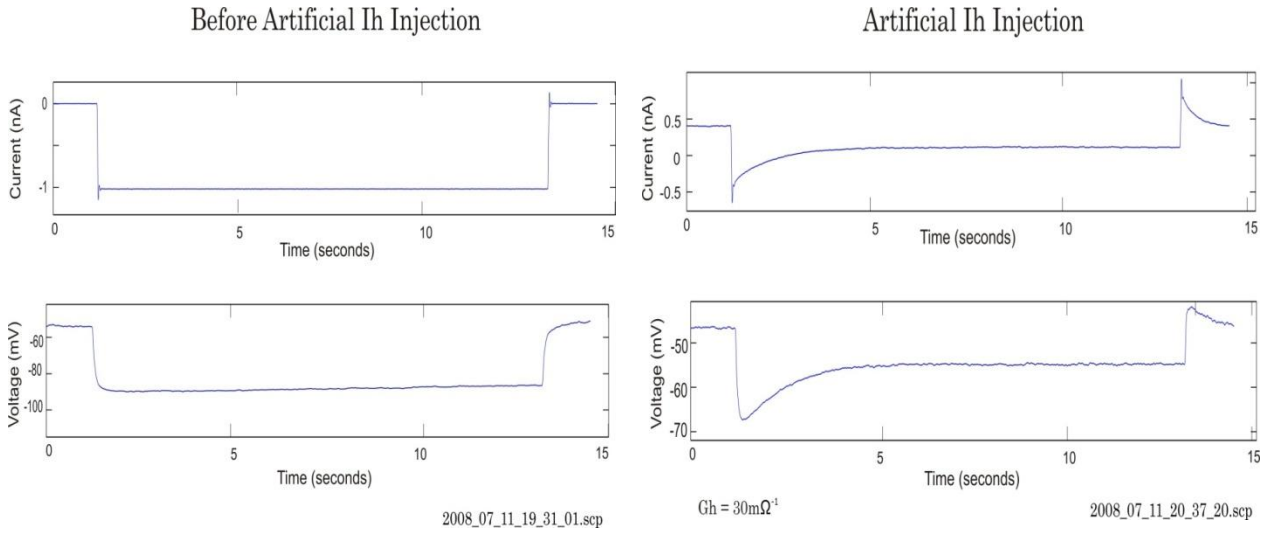

Figure 10: The graph shows the step current injection for the control experiment and variable experiment. In addition, the voltage responses are also shown for before and after the Ih injection.

After injecting the step currents, a zap current was applied for before and after dynamic clamp as observed in figure 11. In figure 11, the voltage response before dynamic clamp is observed where the pyloric neuron hyperpolarized from -30mV to -90mV. In this graph, the biggest change in voltage occurs between 50 seconds and 100 seconds, however this change in voltage is very minimal. On the other hand, the voltage response for after dynamic clamp clearly shows a sign of resonance. The graph appears to have a greater voltage response between 70 seconds and 110 seconds in comparison to the voltage response before dynamic clamp which was minimal.

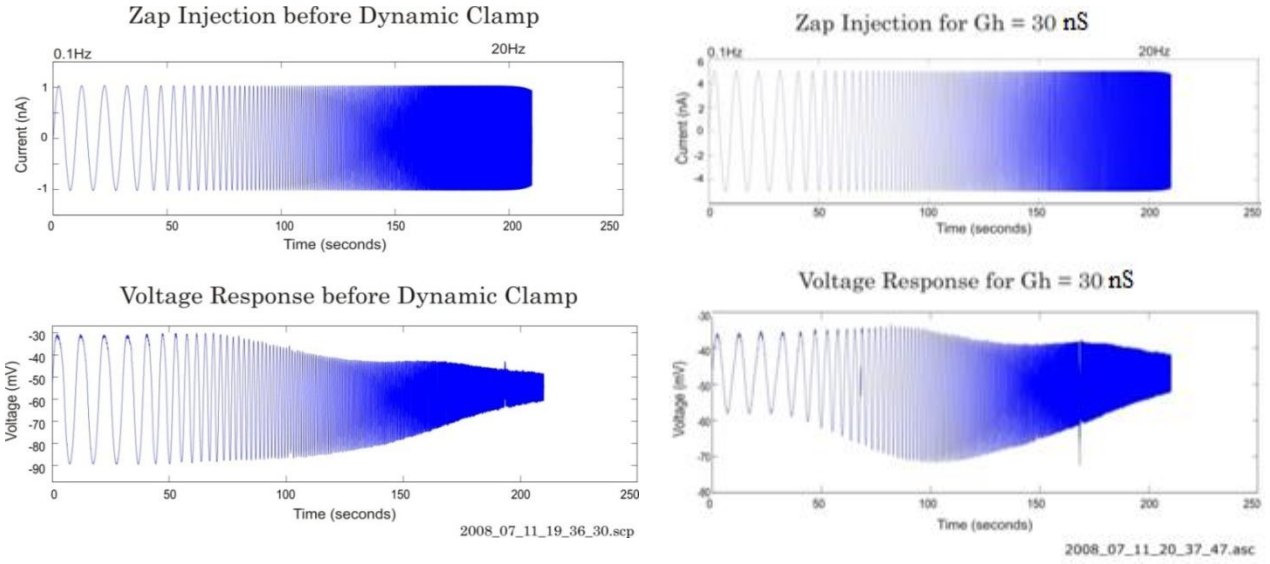

Figure 11: the graphs on the left show the zap injection and voltage response before dynamic clamp. However, the graphs on the right show the zap injection and voltage response after dynamic clamp.

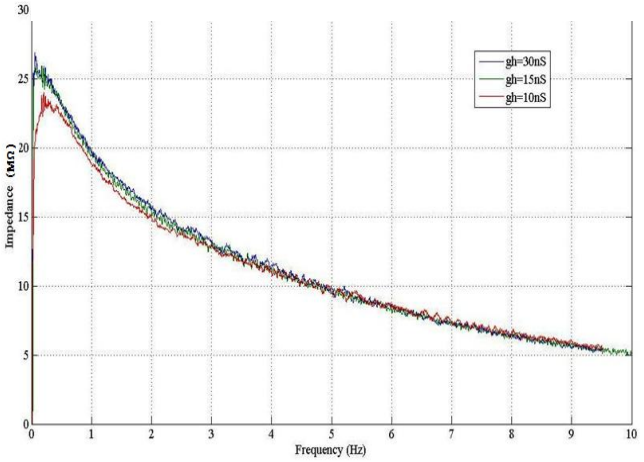

Figure 12: This graphs shows Impedance vs. Frequency using Method2. The first line refers to gh=10nS, the second line refers to gh=15nS and the third line refers to gh=30nS .

Even though it is clearly visible the voltage response with the zap injection after dynamic clamp, the artificial Ih injection of current was applied with different gh conductance. Experimentally, the gh ranged from 10 nS to

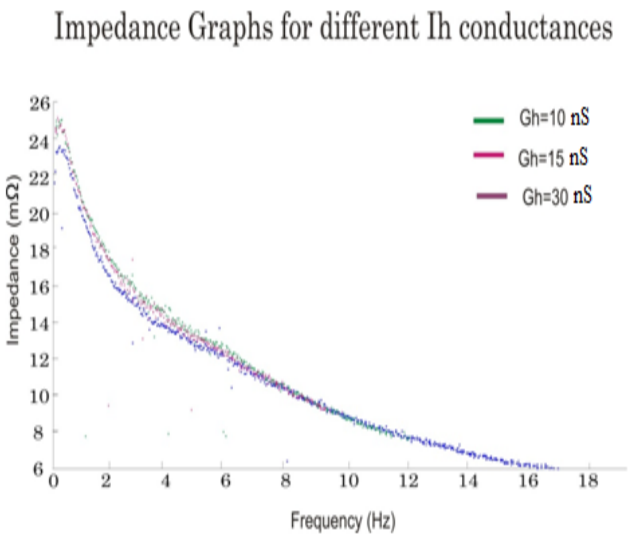

Figure 13: This graph shows the Impedance vs. Frequency using Method1.

30nS and it was observed that as the gh increased, resonance was observed more clearly as shown in figure 12. In addition, there is a higher impedance peak as resonance increases as demonstrated by both Method1 and Method2.

V. The Model

The Hodgkin and Huxley model consists of a set of nonlinear ordinary differential equations that attempts to describe the initiation and propagation of action potentials in neurons (Nelson 2008). In other words, it represents the ion flows in an electrical circuit diagram shown in Figure 1. By using this model, we run different simulations that contribute to the understanding of resonance in a neuron. In addition, we will use parameters similar to those applied in the experiments to be able to compare and discuss the results gathered.

In a simple electrical circuit diagram as showed in Figure 14, the semi-permeable cell membrane separates the interior of the cell from the extracellular liquid therefore it acts as a capacitor. In addition, there are ions movements across the membrane due to pumps which for our purposes will be refer as a leakage current (Il) and Ih current, each with its own resistance. In addition, if an input current is injected into the cell, a charge might be added to the capacitor or leak through the channels in the cell membrane. Since there is an active ion transport through the cell membrane, the ion concentration inside the cell is different from that in the extracellular liquid. Consequently, by applying the Nernst equation, the equilibrium potential of each ion can be determined (Peterson 2008).

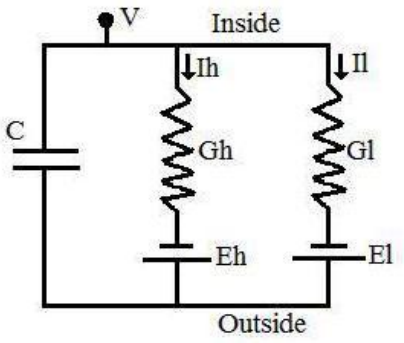

Figure 4: This graph demonstrates the relationship between an electrical circuit and a cell therefore explaining the Hodgkin and Huxley model.

Mathematical equations can be derived to explain the electrical circuit diagram. According to the conservation of electric charge on a piece of membrane, the applied current can be split in a capacitive current which charges the capacitor and other currents which for purposes

of the experiment will only be referred to the leak current and Ih current as shown in equation (1).

$$I_{ex}(t) = I_l(t) + I_h(t) \quad (1)$$

From the definition of capacitance, it is known that:

$$C\frac{dv}{dt} = -\sum I(t) \quad (2)$$

In equation (2), C represents the capacitance and v is the voltage across the capacitor. However, in biological terms, $\frac{dv}{dt}$ is the voltage across the membrane and $\sum I(t)$ is the sum of the ionic currents which pass through the cell membrane.

From Ohm's law, it is known that voltage is current times resistance, consequently equation (3) can be utilized for each ion *c*:

$$I_c = \frac{V_c}{R_c} \quad (3)$$

Since conductance (g) is the reciprocal for resistance, all the ionic currents can be rearranged into the following equation (4).

$$I_c = \frac{1}{R_c}V_c \quad \rightarrow \quad I_c = g_c V_c \quad (4)$$

However, *v* in equation (4) represents the driving force for the ionic flow which is the difference between the ion equilibrium potential and the voltage across the membrane as shown below:

$$I_c = g_c(V - E_c) \quad (5)$$

For purposes of our model, we will be only considering the leakage current and the Ih current. The leakage current I_l is defined by equation (6); where the leak channels, which account for the permeability of the cell membrane to ions, are represented by a voltage independent conductance (Buchholtz 1992).

$$I_l = g_l (V - E_l) \tag{6}$$

The hyperpolarized activated current I_h is defined in equation (7) and describes the voltage gated ion channels represented by a nonlinear conductance g_h therefore the function is voltage and time dependent.

$$I_h = g_h \, r \, (V - E_h) \tag{7}$$

In addition, if the I_h current has its entire ion channels open then it will transmit a current with a maximum conductance. However, some of its channels might be blocked therefore, the probability that a channel is open is called an activation variable denoted as *r* whose value ranges from zero to one (Buchholtz 1992). The activation variable which is time dependent is calculated as follows:

$$\frac{dr}{dt} = \frac{r_\infty - r}{\tau} \qquad \tau = \frac{C_r}{1 + e^{(v - v_{kr})/S_{kr}}} \tag{8}$$

$$r_\infty = \frac{1}{1 + e^{(v - v_r)/S_r}} \tag{9}$$

τ represents the time constant or in other words the time course for approaching an equilibrium value in equation (8). Also, V_r is the voltage required to have half of the number of channels open and S_r is simply the slope of the function r_∞ (Buchholtz 1992).

Consequently, the complete Hodgkin Huxley differential equation for the purposes of our model is as follows:

$$C\frac{dv}{dt} = I_{ex} - g_l\,(V - E_l\,) - g_h\,r\,(V - E_h) \tag{10}$$

$$\frac{dr}{dt} = \frac{r_\infty - r}{\tau} \tag{11}$$

The external current applied is simply a sine function representing the exact zap current used experimentally.

The parameters used for this model are given as follows:

Leak Current	**Ih Current**	**Activation Variable**	**Time Constant**
$I_l\ = g_l\,(V - E_l\,)$	$I_h = g_h\,r\,(V - E_h)$	$r_\infty = \frac{1}{1 + e^{(v - v_r)/S_r}}$	$T = \frac{C_r}{1 + e^{(v - v_{kr})/S_{kr}}}$
$g_l\ = 0.1\ \mu S$	$g_h = 0.037\ \mu S$	$v_r = -70\ mV$	$V_{kr}\ = -110\ mV$
$E_l\ = -70\ mV$	E_h = -10 mV	$S_r = 7\ mV$	$S_{kr}\ = -13\ mV$

VI. Model Results

By using numerical methods through a program called XPP, we were able to analyze the results of the differential equation in the Hodgkin and Huxley model. In addition, the software called MATLAB was used to produce the Impedance vs. Frequency graphs showed throughout the paper. Since the experimental data let us to believe that resonance does not exist in the pyloric neuron, we use the model to investigate the reasons for this result. Consequently, it is believed that the hyperpolarized current found in the pyloric neuron it is not strong enough to produce resonance. Therefore, one of the factors that might affect the strength of the I_h current which is conductance (G_h).

By analyzing equation (7) for the hyperpolarized current, it can be deducted mathematically that an increment in G_h will lead to a stronger I_h current. Consequently, the predicted model was used to test this idea by analyzing the different voltage responses according to the corresponding G_h that ranged from from 0 µS to 0.4 µS. Most importantly, the impedance vs. frequency graphs for the different G_h was calculated as observed in Figure 15. It's clearly seen that when G_h is 0 µS there is no visible impedance peak.

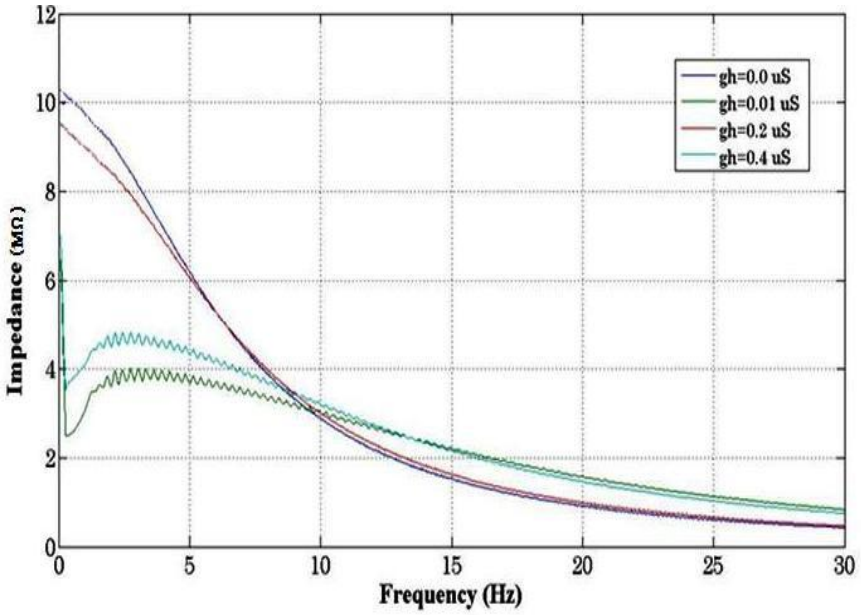

Figure 15: Impedance vs. Frequency graph for changes in Ih conductance.

As expected, resonance is not visible since when G_h is 0 µS, the Ih current is very weak and almost non-existing. As a result when conductance was increased, resonance becomes more visible, especially when G_h is 0.4 µS as showed in Figure 15.

Through the model, it was observed that Ih conductance is not the only factor that affects resonance. By considering different values of τ (Ih time constant), it was determined that τ changes the resonant frequency. For instance, in Figure 16 the values of τ were decreased by decreasing the rate constant (C_r) which ranged from 375 s to 3000 s. When the rate constant is at 3000 s, the resonant frequency is approximately 3Hz however, when rate constant is 375 s the resonant frequency is approximately 10 Hz. Consequently, as τ decreases, the resonant frequency increases thereby observing a right shift of the resonance graph.

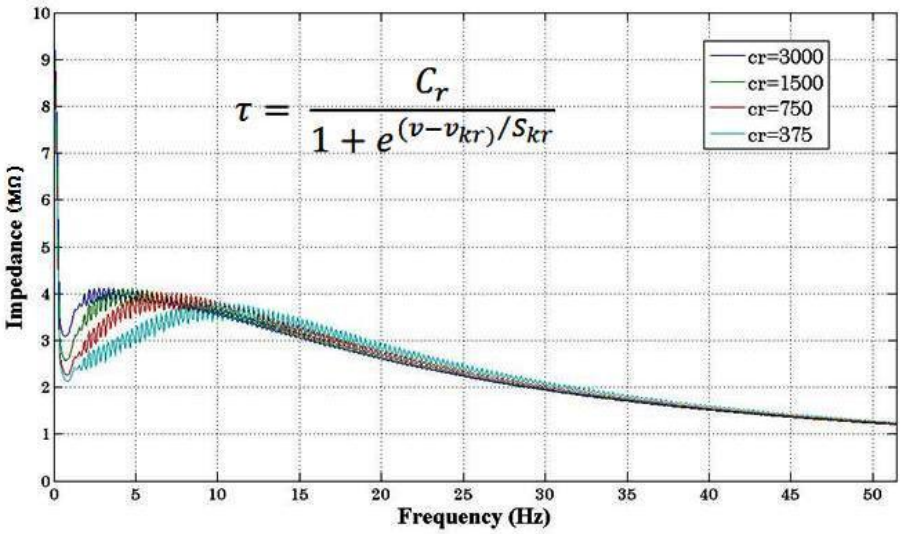

Figure 16: Impedance vs. Frequency graph for different values of τ

In addition to changing the Ih conductance and time constant, changes in capacitance were also tested using the Hodgkin and Huxley model. By using the model, the Impedance vs.

Frequency graphs were plotted for different capacitance values that ranged from 10nF to 60nF as observed in Figure 17.

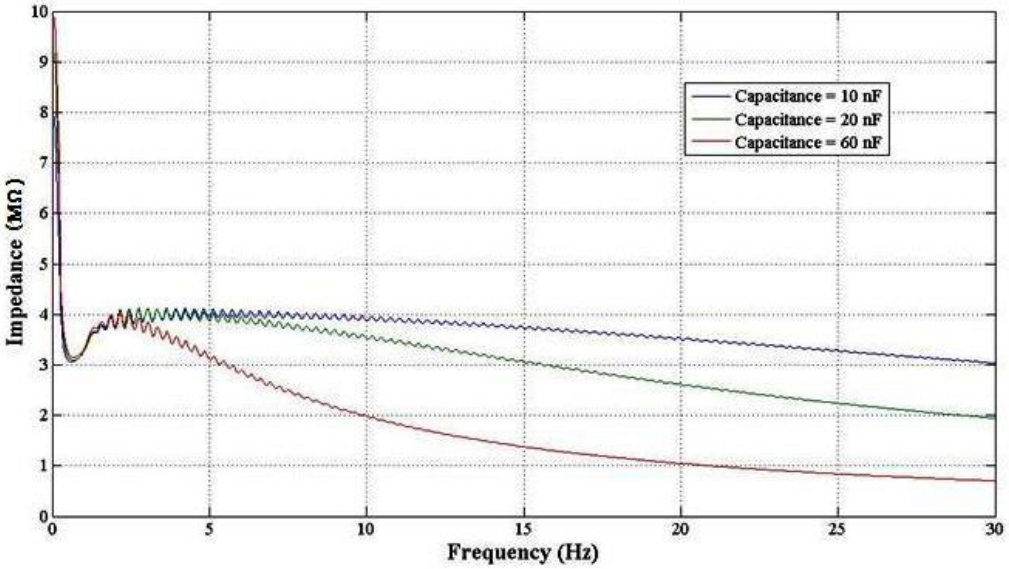

Figure 17: Impedance vs. Frequency graph for changes in Capacitance.

As predicted, the resonant frequency does not change when changes in capacitance are made. However, as capacitance increases, there is a better filter at higher frequencies thus the resonance peak is observed more clearly.

VII. Discussion

Through many studies, it has been discovered that resonance exists among many neurons found in the STG. However, not many studies regarding resonance have been performed on the pyloric neuron. As a result, our project focused on determining the existence of resonance in this specific cell. As mentioned before, resonance is a property that characterizes the frequency at which neurons respond best to inputs of injected current. Consequently, if a neuron exhibits a resonant property then there is a specific frequency at which the neuron will have a higher impedance value.

By performing many experiments on the pyloric neuron it was concluded that resonance was not visible in this cell. One of the reasons for not being able to find resonance is that the Ih current found in py is not strong enough. A strong Ih current is needed for the cell to be able to block the low frequencies thus acting as a high pass filter. However, since this neuron's active property is not very visible then the voltage response encountered upon the zap injections was minimal therefore explaining the absence of resonance. These conclusions were confirmed by performing the dynamic clamp technique since an artificial Ih current was injected to the neuron and as a result resonance emerged.

In addition, a model was created to explore the factors that influenced resonance and thereby explain the reasons for not finding a resonant frequency in the PY neuron. It was observed that the conductance found in the natural neuron might be too low since by increasing the Ih conductance experimentally and through the model, resonance became more visible. Also, it is known that the PY neuron is relatively very small in size compared to the other neurons found in the STG. Consequently, the cell's size was increased by increasing the capacitance in the model. It was observed that resonant frequency of the cell did not change however resonance

became more visible for larger values in capacitance since there was a better filter of the voltage response for higher frequencies. As a result, the absence of resonance in the PY neuron can be explained due to the cell being very small in size. Finally, the PY neuron is a follower neuron therefore it might not have a preferred resonant frequency since it receives signals from AB and LP neuron.

VIII. Matlab Script

A. Script for finding resonance using Method2

```
function [zf]=resonantdetectA(dat, ChannelCl, ChannelCs)

% the version of resonantdetect for loaded ascii files%

sample_rate = 4000;
% Reading the files %
Y=dat(:,ChannelCs).*100;
X=dat(:,ChannelCl).*10;

% Calculation of power spectrums of data %
z1=fft(Y);
z2=fft(X);
PX = abs(z1.*conj(z1)/size(z1,1));
f=(0:(size(z1,1)-1))*(sample_rate/size(z1,1));

s1=z1.*conj(z2);
s2=z2.*conj(z2);
zf=s1(1:2000,1)./s2(1:2000,1);

% phasezf=phase(zf(1:500,1));
anglezf=angle(zf(1:2000,1));
zf=abs(zf);

% filtering%
h = fspecial('average', [9 9]);
Afzf = imfilter(zf, h, 'replicate');
% Afzf = imfilter(Afzf, h, 'replicate');
anglezf = imfilter(anglezf, h, 'replicate');

% cd C:\Documents and Settings\UBM\My Documents\MATLAB\MATLABRESULTS;

prompt={'The experiment category :'};
      def={['PD_ZAP']};
      dlgTitle='Type';
      lineNo=1;
      answer=inputdlg(prompt,dlgTitle,lineNo,def);
      answer(1,1),

      ff=f';
zfout = [ff(7:2000,1) Afzf(7:2000,1) anglezf(7:2000,1)];
zfname = ['z' char(answer(1,1))];

      wk1write(zfname,zfout);

% Plots %

figure(3);
subplot(4,1,1), plot(Y);
```

```
tit1=['FFT of the response File '];
subplot(4,1,2), plot(X);
tit3=['FRC by FFT method : File '];
subplot(4,1,3), plot(f(3:2000), Afzf(3:2000)), title(tit3), xlabel('Frequency (Hz)'), title('Impedance'),axis([0 10 5
30]);
subplot(4,1,4), plot(f(3:2000),anglezf(3:2000)), title(tit3), xlabel('Frequency (Hz)'), title('Angle');
Z1=[];
F1=f;
```

B. Script for finding resonance using Method1

```
% find the frequency-response for each cycle

function [amp] = freq_amp(recordfile,channel)

srate=4000;
uptime=[];
out=[];

original=dlmread(recordfile);
original(:,3)=original(:,3)*10;
original(:,4)=original(:,4)*100;

%drop first/end 4000points=1sec
trustart=0;
truend=0;
original=original(trustart*4000+1:size(original,1)-truend*4000,:);


baseline=(max(original(:,channel))+min(original(:,channel)))/2

shiftbase=original(:,channel)-baseline;

for i=1:size(shiftbase,1)-1
   if ((shiftbase(i)<0) && (shiftbase(i+1)>0))
      uptime=[uptime;i];
   end
end

for j=1:size(uptime,1)-1
   t=uptime(j+1)-uptime(j);
   period=t/(srate);
   f=1/period;
   ch1=max(original(uptime(j):uptime(j+1),1))-min(original(uptime(j):uptime(j+1),1));
   ch2=max(original(uptime(j):uptime(j+1),2))-min(original(uptime(j):uptime(j+1),2));
   ch3=max(original(uptime(j):uptime(j+1),3))-min(original(uptime(j):uptime(j+1),3));
   ch4=max(original(uptime(j):uptime(j+1),4))-min(original(uptime(j):uptime(j+1),4));
   out=[out;ch1 ch2 ch3 ch4 f];
%    out=[out;ch1 ch2 ch3 ch4 f uptime(j) uptime(j+1)];
end


if (size(out)~=[0,0])
```

```
out(:,6)=out(:,3)./out(:,1);
%out(:,7)=out(:,4)./out(:,2);
out(:,7)=out(:,4)./out(:,3);

%tital
% newtitle=[strrep(recordfile,'_',':'),', ',num2str(channel),' (',num2str(baseline),'), (',num2str(trustart),',
',num2str(truend),')'];
% suptitle(newtitle)

%reset all plot
%reset all graph
% subplot (3,2,1)
% hold off
% subplot (3,2,2)
% hold off
% subplot (3,2,3)
% hold off
% subplot (3,2,4)
% hold off
% subplot (3,2,5)
% hold off
% subplot (3,2,6)
% hold off

%scatter plot
% subplot (3,2,1)
% scatter(out(:,5),out(:,1),5,'filled')
% title(['1 (',num2str(channel),')'])
%
% subplot (3,2,2)
% scatter(out(:,5),out(:,2),5,'filled')
% title(['2 (',num2str(channel),')'])
%
% subplot (3,2,3)
% scatter(out(:,5),out(:,3),5,'filled')
% title(['3 (',num2str(channel),')'])
%
% subplot (3,2,4)
% scatter(out(:,5),out(:,4),5,'filled')
% title(['4 (',num2str(channel),')'])
%
% subplot (3,2,5)
% scatter(out(:,5),out(:,6),5,'filled')
% title(['3/1 (',num2str(channel),')'])
%
% subplot (3,2,6)
scatter(out(:,5),out(:,7),5,'filled')
% title(['4/2 (',num2str(channel),')'])
%
% save([recordfile,'_',num2str(channel),'_(',num2str(trustart),', ',num2str(truend),').txt'],'out','-ASCII')
% saveas(gcf,[recordfile,'_',num2str(channel),'_(',num2str(trustart),', ',num2str(truend),').jpg'])

figure(10)
subplot(2,1,1)

x=max(length(original(:,3)),1);
```

```
plot((1:x)*.00025, original(:,3))

subplot(2,1,2)

plot((1:x)*.00025, original(:,4))


end

amp=out;
```

C. Script used in XPP model

```
par A=-10 gl=0.1 El=-70 gh=0.037 Eh=-10 vr=-70 Sr=7
par c=20 cr=3000 vkr=-110 skr=-13
par fmax=.01 fmin=0.0001 dur=180000


logval=log(fmax/fmin)/dur
Iex=A*sin(2*pi*(fmin/logval)*(exp(logval*t)-1))-5
aux Ix=Iex


# define currents
#Iex=A*heav(t>10000)*heav(t<140000)
#aux Ix=Iex

Il=gl*(v-El)
Ih=gh*r*(v-Eh)
aux ihx=ih


# define activation fraction of the h current

rinf=1/(1+exp((v-vr)/Sr))
taur=cr/(1+exp((v-vkr)/Skr))

aux rx=r
aux rinfx=rinf


# ODEs
v'=(Iex-Il-Ih)/c
r'=(rinf-r)/taur

@ total=60000 dt=1,xlo=0,xhi=180000,ylo=-70,yhi=-40

@ total=180000 dt=1,xlo=0,xhi=180000,ylo=-90,yhi=-30
@ bounds=10000000

init v=-60 r=0.3280024747199

done
```

References

Buchholtz, Frank, & Golowasch, Jorge, & Epstein, Irving, & Marder, Eve. "Mathematical Model of an Identified Stomatogastric Ganglion Neuron." Journal of Neurophysiology 67(1992): 332-340.

Buchholtz, Frank, & Epstein, Irving, & Marder, Eve. "Models of Subthreshold Membrane Resonance in Neocortical Neurons." Journal of Neurophysiology 76(1996): 698-714.

Harris-Warrick, Ronald M., Eve Marder, and Allen I. Selverston, eds. Dynamic Biological Networks : The Stomatogastric Nervous System. New York: MIT P, 1992.

Hutcheon, Bruce, & Yarom, Yosef. "Resonance, oscillation and the intrinsic frequency preferences of neurons." Trends in Neurosciences 23(2000): 216-222.

Kilman, Valerie L., and Eve Marder. "Ultrastructure of the stomatogastric ganglion neuropil of the crab, Cancer borealis." The Journal of Comparative Neurology 374 (1998): 362-75.

Nadim, Farzan. "Software." The STG Lab at Rutgers University and NJIT. 2006 November 1, 2008. http://cancer.rutgers.edu/software/index.html

Nadim, Farzan. "Cancer Borealis." The STG Lab at Rutgers University and NJIT. 2006 November 1, 2008.

http://cancer.rutgers.edu/stg_lab/protocols/cancer_borealis%20saline.htm

Nelson, Mark and Rinsel, John. "The Hodgkin-Huxley Model." November 1, 2008.

http://www.genesis-sim.org/GENESIS/iBoG/iBoGpdf/chapt4.pdf